From Simulations to Measurements: Prototyping an Antenna for Non-Linear Applications at Sub-THz Frequencies

DONNAN, RS; Pigeon, M; Sushko, O; Kreouzis, T; Parini, C; Wang, H; Alderman, B; Huggard, P; Dubrovka, R

From Simulations to Measurements: Prototyping an Antenna for Non-Linear Applications at Sub-THz Frequencies

Journal:	*IET Microwaves, Antennas & Propagation*
Manuscript ID	MAP-SI-2016-0392.R1
Manuscript Type:	Research Paper
Date Submitted by the Author:	n/a

Complete List of Authors:	Pigeon, Melusine; Queen Mary University of London, School of Electronic Engineering and Computer Science Sushko, Oleksandr; Queen Mary University of London, School of Electronic Engineering and Computer Science Donnan, Robert; Queen Mary University of London, School of Electronic Engineering and Computer Science Kreouzis, T. ; Queen Mary University of London, Physics Parini, Clive; Queen Mary University of London, Electronic Engineering and Computer Science Wang, Hui; STFC Rutherford Appleton Laboratory, RAL Space Alderman, Byron; STFC Rutherford Appleton Laboratory, RAL Space Huggard, Peter; STFC Rutherford Appleton Laboratory, RAL Space; Dubrovka, Rostyslav; Queen Mary University of London, School of Electronic Engineering and Computer Science

Keyword:	FREQUENCY MULTIPLIERS, MILLIMETRE WAVE DEVICES, SCHOTTKY DIODES

From Simulations to Measurements: Prototyping an Antenna for Non-Linear Applications at Sub-THz Frequencies

M. Pigeon[1], O. Sushko[1], R. S. Donnan[1], T. Kreouzis[2], C. G. Parini[1], H. Wang[3], B. Alderman[3], P. G. Huggard[3], R. Dubrovka[1*]

[1] School of Electronic Engineering and Computer Science, Queen Mary University of London, Mile End Road, London E1 4NS, UK,
[2] School of Physics and Astronomy, Queen Mary University of London, Mile End Road, London E1 4NS, UK
[3] RAL Space, STFC Rutherford Appleton Laboratory, Didcot OX11 0QX, UK
*r.dubrovka@qmul.ac.uk

Abstract: The simulated characterisation and tuning of prototype antennas prior to manufacture is described in this article. The antennas incorporate Schottky diodes so as to frequency triple incident sub-THz power. Such a dual frequency, nonlinear, device has been called a multenna. A metrology is outlined for ease of multiple measurements to permit exploring scenarios of multenna element design. Four options are optimally oriented and assembled onto an appropriately dimensioned tile substrate to minimise mutual coupling during characterisation of each element individually. Transmission measurements of the multennas are performed at 100 and 300 GHz: an example of resonant behaviour is presented.

1. Introduction

Unlike X-rays, non-ionising terahertz (THz) radiation is not known to damage organic material. Therefore over the last decades many applications have been studied using THz radiation, namely: spectroscopy; bio-sensing; medical and pharmaceutical applications; and potential industrial and security applications [1-6]. However, the full exploitation of this sub-band of the electromagnetic spectrum is currently limited by the availability of wideband, coherent, THz sources. As summarized in [7], different technologies can be used to create THz sources. The most common technique is to frequency multiply from a lower frequency electronic source using a non-linear, usually Schottky diode-based, multiplier [8]. The key limitation of this is that the maximum output power decreases with increasing frequency i.e., W at 100s MHz dropping to μW at THz. Another limitation is that antennas, and associated RF circuitry, are difficult to miniaturize for operation at THz frequencies. Nevertheless, frequency multipliers are convenient because they are phase-lockable and frequency agile, do not need cryogenic cooling, are robust and compact, and have a long operational lifetime. Even so, state-of-the-art solid-state Schottky multiplier chains are based on waveguide technology that is bulky [9] so that in an array format, individual tuning of elements is impracticable. In view of this, our development route is to create a quasi-optical (QO) multiplier array. No waveguides are needed and the multiplied outputs from elemental solid-state devices are coherently combined. Non–linear devices, GaAs Schottky diodes, are coupled to antenna array elements whose outputs are *spatially* combined (as a coherent planar sum), as opposed to conventional

(longitudinal) power combining [10, 11]. The main advantages of a QO multiplier array are the lateral compactness of the device, built-in frequency and polarization control, simpler impedance matching, reduced ohmic losses and, as each element contributes a small part of the total power, there is reduced risk of thermal breakdown. Previous studies on QO diode-based multipliers are based on simplistic multiplier elements like wire grids [12], waveguide slots [13], bow-tie antennas [14] or patch antennas [15]. Most of these studies used the harmonic balance technique to design QO multipliers, and only a limited amount of work includes full-wave simulations of the QO multiplier with a detailed diode structure [13]. This work suggests an alternative design of the diode-coupled antenna element based on a ring-with-stubs structure, which is optimized to match the diode impedance at both fundamental and 3rd harmonic. The majority of the previous studies use HFSS in combination with ADS for full-wave EM analysis of the structures [16]. This work uses the built-in FDTD method of CST with incorporation of lumped elements for analysis of the multenna. This method has been rarely adopted previously, and only for multipliers below 20 GHz [13].

In this article we report on a slot-ring antenna loaded with a frequency tripling Schottky diode to form the basis of a THz source. This hybrid device is called a 'multenna'. The multenna, which has met performance specifications in simulation, is manifest as a completely planar, printable, integrated device [17]. To go from simulation to measurement, a prototype of the multenna has been developed. The key constraint to its manufacture is its operating size. The size concern is firstly addressed and then the apparatus for experimental verification is covered. In summary, this new multenna structure is proposed in order to meet ultimately both antenna specifications and, manufacture and measurement requirements of a compact, coherent, high-power (~ 10s mW), THz source. This paper also shows that the lumped element FDTD method can be utilized for sub-THz multipliers and results of simulation and measurements agree. In contrast to previous studies, this paper shows both passive (S_{21} transmission – to test resonant behavior) and active (to characterize tripling performance) measurements of the tripler.

2. The multenna

As described by Pigeon *et al.* [17, 18], the multenna is an antenna operating at two different frequencies; here 100 and 300 GHz. This is possible due to the incorporation in the antenna design of a GaAs diode acting as a tripler. The bespoke single Schottky diode used in each device is fabricated at the Rutherford Appleton Laboratory (RAL). The multennas are photolithographically defined on a 2-3 μm thick gold layer that is deposited by a combination of sputtering and electroplating on a 75 μm thick fused quartz substrate. This is a standard process used for forming microstrip filters and transmission lines in waveguide mixers and multipliers at RAL [19]. The quartz substrate is then mounted on a PTFE holder

and the discrete diode chips are soldered in place. This antenna is based on a slot-ring design. It has been optimized for the generation of a third harmonic (not discussed in this article). Consequently, the length of the perimeter of the antenna is around 1 λ of the lower frequency (100 GHz). The antenna has been iteratively tuned to match the specific impedance of the diode at both 100 and 300 GHz. This increases the power available to drive the diode and optimised the generated third harmonic power.

The planar gold slot multenna is contained on a fused quartz dielectric square with a side-length of the metallised area of 1 mm. One of the designs of the multenna that meet specifications in fabrication tolerances is shown in Fig. 1.

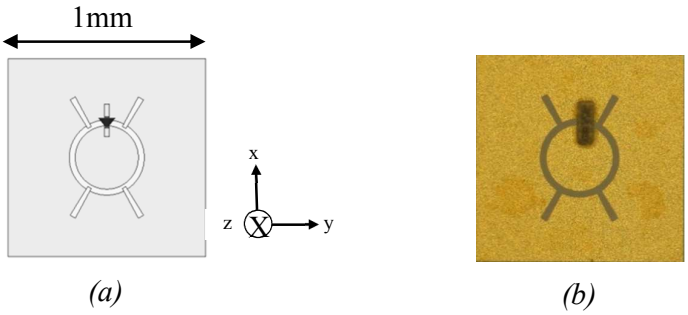

Fig. 1*: One possible design of the multenna, termed "ET": it is a modified slot ring with stubs to enhance third harmonic yield. (a) Shows a schematic of the antenna and, (b) is a photograph of the manufactured antenna. The grey rectangle in (b) is the chip that carries the Schottky diode.*

This specific design uses the well-known techniques of deploying quarter-wavelength stubs (in the minima of the field distribution of third harmonic) to create nulls in the electric field distribution at 300 GHz, thereby enhancing the yield of the third harmonic without disturbing the field distribution of the fundamental [18]. This design is dubbed "ET" and the reflection coefficient results obtained for it in simulation are shown in Table 1. Note that multenna matching is of a resonance nature, so that the multenna is poorly matched at other frequencies apart from at 0.1 and 0.3 THz. Such low reflection coefficients indicate that most of the energy is transmitted through the multenna, maximizing S_{21} at these operating frequencies.

Table 1. S_{11} parameters of the "ET" multenna

Frequency (THz)	ET (dB)
0.1	-10.28
0.3	-22.70

While the size of the slot-ring is consistent for the frequency studied, it nonetheless proves impracticably small; i.e. the element is difficult to manipulate for soldering and measurement and some peculiarities may result. The slightly off-centred diode seen in Fig 1b is one such example.

Four different prototype multennas have been designed. One example of each was defined photolithographically on a 20 x 20 mm^2 tile of quartz, Fig 2. For ease of handling and test, a choice was made not to dice each prototype prior to soldering the diodes. Rather, the prototypes are retained in the array format throughout: it will be shown below that this does not adversely affect the testing of the individual elements.

3. The 4-element Prototype

Of the 20 x 20 mm^2 area of the tile upon which the prototype multenna elements are set, only the central 15 x 15 mm^2 area is 'active'. The corresponding footprint-region of the antenna elements is highlighted in Fig. 2. The outer area provides a margin for safe handling. The prototype multennas' centres are separated by a minimum of 7.5 mm, corresponding to 7.5λ at 300 GHz and 2.5λ at 100 GHz.

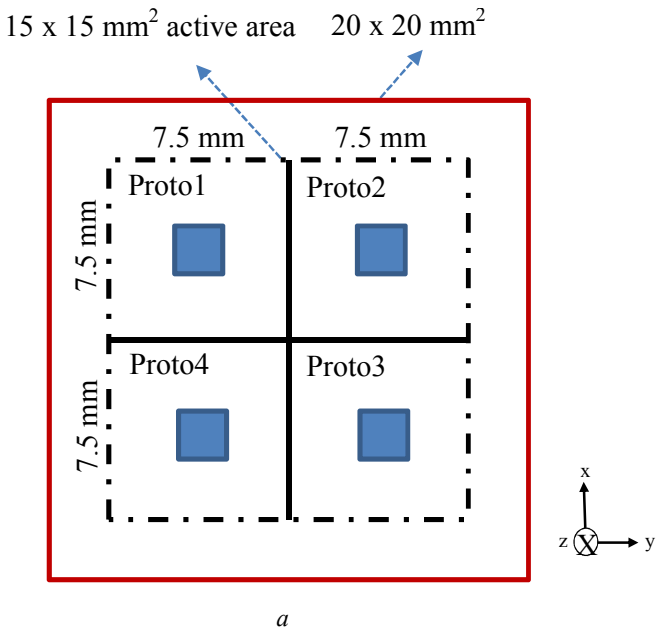

a

***Fig. 2**: Schematic of the quartz tile upon which four prototypes of the multenna are set.*

From the point-of-view of a given multenna, the size of its substrate has been markedly increased from 1 (initial simulations were performed for 1 mm^2 multenna) to 7.5 mm, or 10 mm if the border to the next multenna is considered. Even so, to further guarantee no unwanted coupling between prototypes, another simple decoupling feature is added to the design, as covered in section 3.2.

3.1 Impact of the substrate size-extension on multenna performance.

The increase of the antennas' sizes concerns only their quartz substrate. The 1 mm^2 conductive part remains fixed and the 7.5 fold increase in substrate does not affect the radiating performance. The impedance of the antenna in both cases has been carefully checked to ensure the matching remains unchanged over the operating band. Comparative results of the real and imaginary parts of the input impedances for the "ET" multenna are shown in Fig 3.

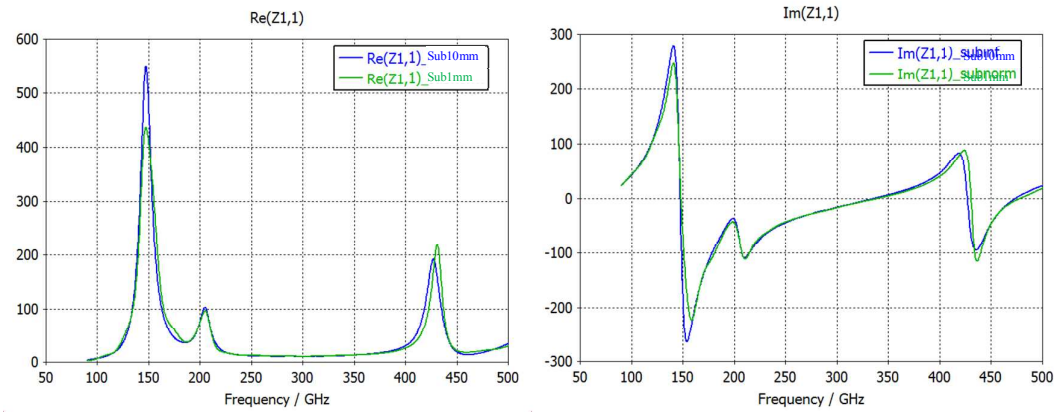

a *b*

***Fig. 3**: a) real and b) imaginary parts of the input impedance of the antenna for the case of a 1 x 1 mm^2 (green), and a 10 x 10 mm^2 (blue), substrate area.*

Even if there are slight differences between the results of a quasi-infinite substrate area and that of a 1 mm^2 area, the impedances, specifically at 100 and 300 GHz, are very close and stay within a few ohms, as shown in Table 2.

Table 2: Input impedances of the multenna for the cases of substrate areas being 1 and 10 mm^2 at 100 and 300 GHz.

Frequency (GHz)	1 mm^2 substrate	10 mm^2 substrate
100	7.2 + j43.7	7.3 + j42.6
300	10.8 - j16.9	10.8 - j16.2

3.2 Decoupling elements

A further reduction in coupling is ensured by orienting multennas such that nearest neighbours couple to orthogonal electromagnetic field polarisations. With reference to Fig. 1, the main polarization of the slot-ring is along the direction of the diode, i.e. the x-axis. Considering Fig. 2, if multenna #1 is polarized along the x-axis, then so is device #3, with #2 and #4 are polarized along the orthogonal y-axis, as shown in Fig 4.

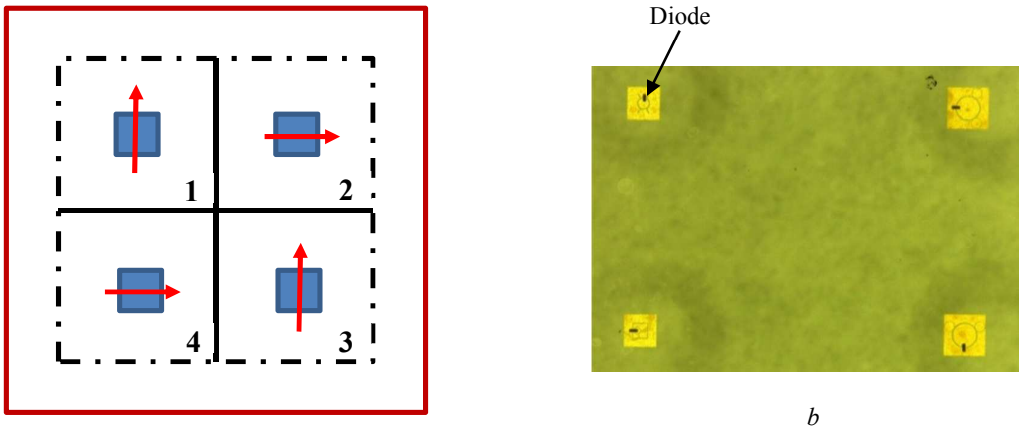

a *b*

***Fig. 4**: a) Orientation for the polarization of the **E**-field for each prototype on the quartz tile and b) the actual display on the quartz tile with diodes (black rectangles), indicating the polarization orientation.*

The final simulation results on coupling between the elements of this "array" are shown in Fig. 5. Simulations are performed using time-domain solver of CST Microwave studio.

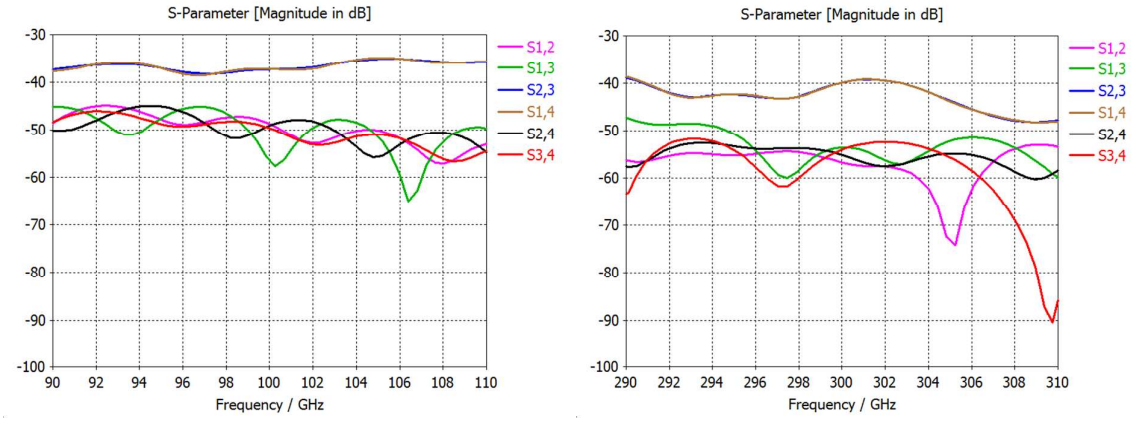

a *b*

***Fig. 5**: S parameters for each multenna prototype on the tile a) at 100 GHz and b) 300 GHz.*

It is clear from the graph that the coupling between elements is always below -30 dB and so they may be practically considered as isolated. It is observed that the isolation between elements 1 and 2 or 1 and 4 is stronger, i.e. ~ -50 dB, than for 1 and 3, ~ -40 dB, which are diagonally displaced. This is explained by the difference of polarization between neighbouring elements, unlike diagonal elements. In more detail simulation results at the two frequencies of interest (100 and 300 GHz) are presented in Table 3.

Table 3: Transmission coefficients (in dB) between different multenna elements on the same tile at 100 and 300 GHz.

	100 GHz		300 GHz	
Isolation	Co-polarisation configuration	Cross-polarisation configuration	Co-polarisation configuration	Cross-polarisation configuration
S_{12}	-32.3	-48.7	-35.3	-56.7
S_{13}	-37.2	-37.3	-40.3	-39.9
S_{14}	-43.4	-56.3	-45.7	-53.5
S_{23}	-43.4	-49.1	-45.7	-55.1
S_{24}	-37.2	-37.4	-40.3	-39.9
S_{34}	-32.9	-49.6	-35.8	-54

With the cross-polarisation configuration an added isolation of about 20 dB is gained. The isolation is improved from between -6.0 and -21.4 dB between neighbouring elements. Horizontal isolation (S_{12} and S_{34}) is better than vertical (S_{14} and S_{23}). Isolation between neighbouring vertical elements is already low without mutual orthogonal polarisation states, approximately -43 dB, and so does not need enhancement. No change is noticed between the diagonal elements S_{13} and S_{24}. This follows since each share a common polarisation state. Even with the distance between neighbouring elements greater than 2λ at 100 GHz and 6 λ at 300 GHz, the change of polarization state between these elements still affects their mutual coupling.

3.3 Measurement using the optical table

In preparation for characterisation the tile is placed in a rotating holder on the optical measurement bench: Fig. 6.

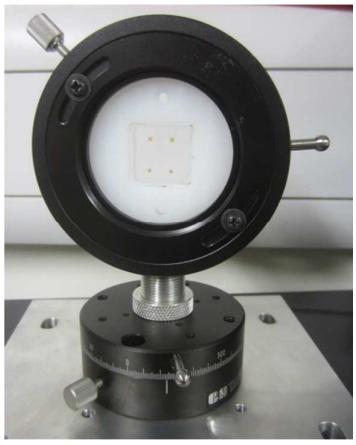

Fig. 6: *The sample with four multennas on a quartz tile fixed in the rotating holder.*

The holder is aligned with respect to the optical system beam waist (see below), so that only the multenna in upper left-hand quadrant of the tile is irradiated. In the initial configuration, prototype 1 is

illuminated according to its polarization configuration. Prototype 2 is brought into the beam by rotating the holder by 90° in the plane of multenna; so each prototype is considered in turn, as shown in Fig 7.

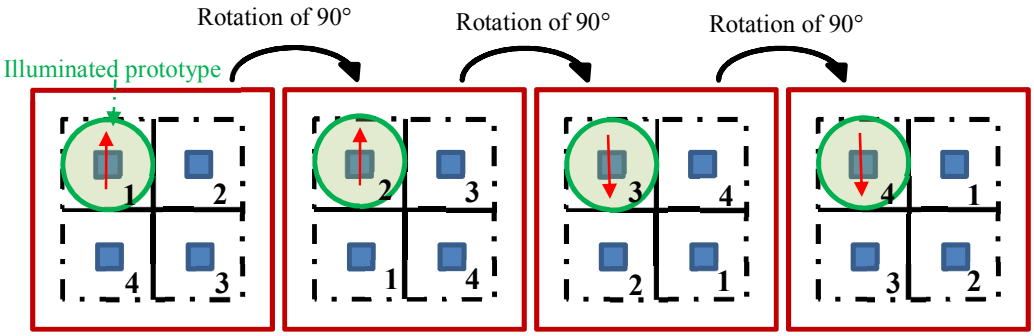

Fig. 7: *The measurement procedure for characterising each prototype antenna in turn for a given polarisation condition by rotating the holder of the tile.*

4. Measurement results

Initially, free space transmission properties of the multennas are tested separately at 100 and 300 GHz. A conventional Z-bench, Fig. 8, is used to acquire S_{21} transmission data over the WR-10 and WR-3 waveguide bands. The associated VNA's frequency extender heads (shown in blue), are controlled by a mm-wave module driven by the network analyser. The heads' waveguide ports are coupled to free-space by corrugated feedhorns. A pair of off-axis ellipsoidal mirrors collimates radiation onto an inner-pair of short focal length mirrors at whose common focal point the sample is placed. The beam-waist at the focus is 4.5 mm and 3 mm at 100 and 300 GHz respectively, while the multenna's metallised area is only 1 mm^2. To illuminate only one of the four multennas, a 3 mm diameter iris is placed 2 mm before the multenna. 3 mm is chosen as a compromise between allowing sufficient illumination and still capturing the multenna signature (a smaller diameter would also make alignment more problematic).

Fig. 9 shows the measured amplitude and phase of S_{21} for ET multenna element over respective waveguide bands. The measurement conditions for Fig. 9 a) and b) are identical, except for the change of the multiplier heads (shown in blue in Fig. 8), for WR-3 and WR-10 bands, respectively. Note that beam parameters and SNR of WR-3 and WR-10 heads are different. Free space S_{21} transmission coefficient served as a reference and was normalized to zero before each reading. The free space S_{21} transmission coefficient served as a reference and was normalized to zero before each reading. The plots in Fig. 9 are obtained by subtracting the quartz transmission from the multenna-on-quartz transmission to display the actual multenna signature. Strictly speaking such a subtraction would not result in a pure multenna response due to the effect of Fabry-Perot (FP) reflections within the substrate. The total contribution of these internal reflections is different for quartz and multenna-on-quartz scenarios. However following such

a procedure still provides a reasonable approximation of the multenna response, since the response is dominated by the transmission of the bare quartz. The procedure of mathematical elimination of substrate response from multenna readings is done only to check the resonance behaviour of the multenna; when evaluating the tripling performance of the multenna such approach is not needed. The trace at 100 GHz is noisier than at 300 GHz since the iris aperture obscures a larger portion of the beam, thus reducing the signal to noise ratio. At the resonance frequency, amplitude reaches an extremum and phase undergoes its most rapid change. In the WR-10 band a clear transmission resonance is present at ~103.5 GHz. It deviates from the modeled 100 GHz center-frequency within acceptable limits, probably due to uncertainties in material properties used in simulations. On the other hand, the broader transmission peak at 300 GHz, despite the nearly-flat phase curve, is also an indication of multenna resonance. As discussed above, the multenna structure is optimized for a low reflection coefficient (or equivalently a transmission peak) at both operating frequencies. Thus, maxima in transmission at 100 and 300 GHz are expected and agree with simulations.

The resonances shown in Fig. 9 have a low Q-factor for two main reasons: (i) only part of the signal is transmitted through to the multenna; the remainder spills around it, thereby muting the resonant response; (ii) the multenna is loaded with the (non-linear) capacitive Schottky diode, which introduces losses to the circuit, thereby lowering the Q-factor. Despite the fact that numerical optimization of the multenna includes detail of the diode structure, it is still challenging to feed accurate material properties to the solver, particularly at 300 GHz.

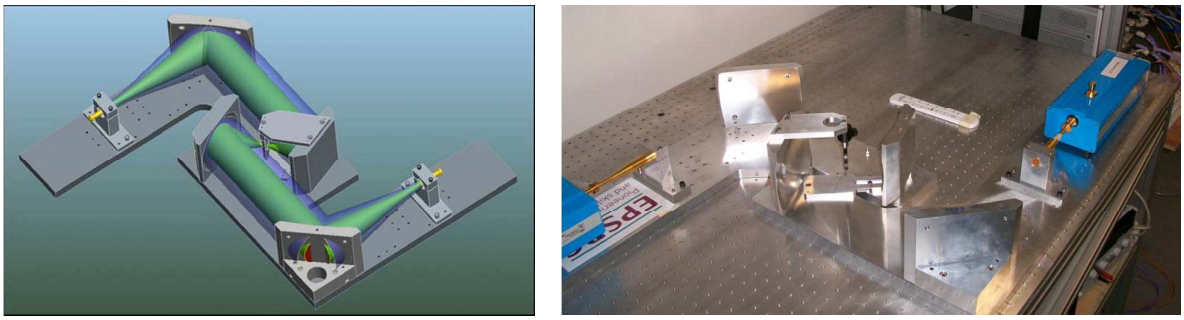

Fig. 8*: Schematics (left) and a picture (right) of the quasi-optical Z-bench incorporating an inner pair of confocal mirrors braced by off-axis ellipsoidal coupling mirrors.*

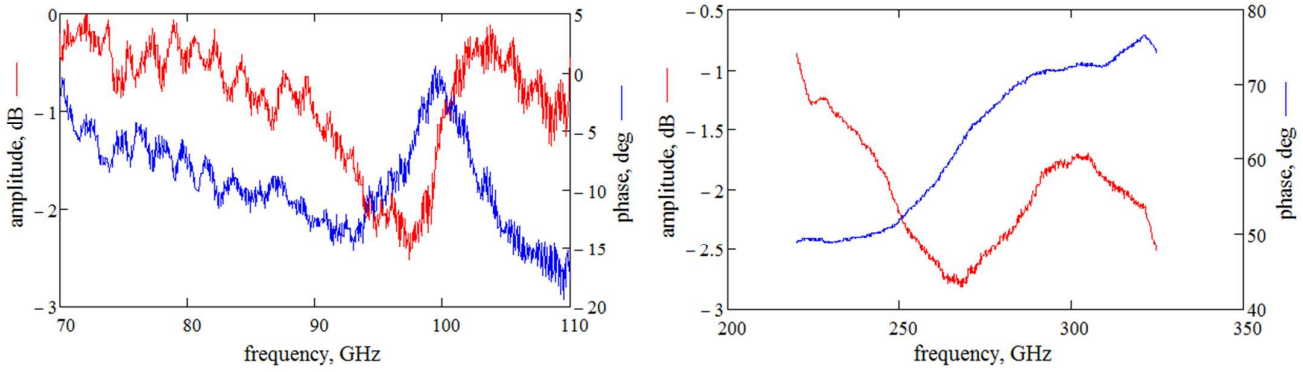

Fig. 9: *Transmission measurements of the single multenna element in WR-10 and WR-3 waveguide bands normalised to the corresponding transmission of the quartz dielectric. Red lines show amplitude data, blue indicates phase.*

For the characterization of the tripling action of the multenna, a clinotron mm-wave oscillator source, tuneable over 93 – 100 GHz, is used to feed the multenna at its ≈100 GHz fundamental resonance: Fig 9 [20]. The clinotron's WR-10 output is coupled to an ultra-Gaussian corrugated feed-horn to provide both a low VSWR (essential for clinotron stability), and a high gain. Radar absorbing material is placed to form a conduit between horn and waveguide attenuator in order to suppress multipath effects. Radiation is also coupled by matched feedhorns to the tuneable waveguide attenuator, which can handle a maximum power of 70 mW. Since typical output power of the clinotron oscillator is a few Watts, an appropriate source-separation introduces free-space loss to prevent overloading of the attenuator. A feed-horn at the output of the attenuator efficiently couples radiation to the first of a confocal pair of mirrors. This mirror is ellipsoidal with a focal length of 250 mm; the second is a 100 mm focal length, off-axis, ellipsoid. The combination of these works to control the projection of the beam-waist over a given multenna element. The emerging field from the frequency tripling multenna is detected by the PNA-driven mm-wave module operating in the WR-3 band (220 – 325 GHz), with a corrugated receive horn. The schematic of the measurement setup for testing the multenna performance is shown in Fig. 10.

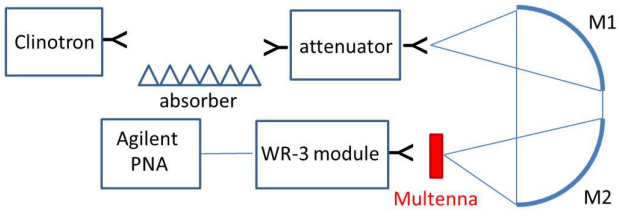

Fig. 10*: Schematic of the measurement setup for testing of the frequency tripling performance of the multenna*

The initial measurements, performed using the setup in Fig. 10, have shown the multenna to function as a tripler. Achievable simulated efficiency of unbiased diode-based triplers in this frequency domain is

approximately 7% [21]. However, efficiency obtained for the multenna, calculated as the ratio of generated power at 300 GHz to the incident power at 100 GHz, is about 3 orders of magnitude lower than expected. One of the reasons for lower efficiency measured in this study is insufficient excitation power (1-2 mW). Also QO multiplier circuits normally have input and output matching dielectric plates, which enhance the output power several times [14]. These tuning slabs, as well as 100 GHz and 300 GHz bandpass filters, were not used in the measurements. Lastly, possible errors in alignment of the multenna with the beam axis and the diode on the multenna itself (a slight asymmetry in diode position as seen in Fig. 1b), could cause lower efficiency. Further work is aimed to resolve these issues.

5. Conclusions

In order to verify the simulated performance of a multenna, several practical modifications are made the our initial fabrication and measurement procedure as a prerequisite to the development of a new, coherent, THz source, based upon spatial power-combining of elemental beams. The different antenna prototypes under study are defined on a shared substrate tile, since separately they are small (area ~ 1 mm^2) and therefore hard to manipulate. The common substrate increases the effective substrate area of each element by a factor of 10. This change is retro-simulated and the differences in input impedance of each element are found to be minimal. To ensure that each prototype is isolated from its neighbours on the common tile, the distance between elements is maximised and only four elements are placed per tile. Further isolation is engineered by orthogonally setting the polarization state of each element with respect to its neighbour. A 90° rotation of the multenna-holder allows each prototype multenna element to be characterised in turn. Transmission measurements are performed showing the resonant nature of the multenna and its suitability for operation as a tripler. The next prototypes are to be fabricated on completely gold-plated substrates, in contrast to just patches in this study. This will avoid leakage of radiation around the multenna. The experimental setup for testing the tripling performance of a multenna is described. Initial characterization of tripling efficiency is performed and the multenna is shown to triple the incident signal. Future work is to be directed on the optimization of the output power by adding matching slabs, investigation of power dependence of the multenna yield and precise alignment of the multenna with respect to the plane of polarisation of Tx.

6. Acknowledgment

The authors gratefully acknowledged the support of the Engineering and Physical Sciences Research Council, UK, under grant number EP/K038125/1.

7. References

[1] Siegel, P. H.: “Terahertz Technology”, IEEE Trans. MTT, 2002, 50, pp. 910-928 .

[2] Tonouchi, M.: “Cutting-edge terahertz technology”, Nature Photonics, 2007, 1, pp. 97-105.

[3] Siegel, P. H.: “Terahertz technology in biology and medicine”, IEEE Trans. MTT, 2004, 52, pp. 2438-2447.

[4] Kemp, M. C. *et al*.: “Security applications of terahertz technology”, Proceedings of SPIE 5070, Orlando, USA, August 2003, 44.

[5] McIntosh, A. I. *et al*.: “Terahertz Spectroscopy: A powerful new tool for the chemical sciences?”, Chem. Soc. Rev., 2012, 41 (6), pp. 2072 – 2082.

[6] Parini, C., Donnan, R.: “Observational science at millimetre wavelengths: imaging, imagining and exciting”, Proc. of LAPC, Loughborough, UK, November 2010, pp. 13 – 20.

[7] Chattopadhyay, G.: “Technology , capabilities and performance of low power terahertz sources”, IEEE Trans. Terahertz Sci. & Technol. 2011, 1, (1), pp. 33-53.

[8] Maestrini, A., *et al*.: “A 540-640-GHz high-efficiency four-anode frequency tripler”, IEEE Trans. MTT, 2010 53 (9), pp. 2835-2843.

[9] Ward, J. S., Chattopadhyay, G., Gill, J., Javadi, H., Lee, C., Lin, R., Maestrini, A., Maiwald, F., Mehdi, I., Schlecht, E., and Siegel, P. H.: “Tuneable broadband frequency-multiplied terahertz sources”, proc. 33rd Int. Conf. Infrared, Millimeter and Terahertz Waves, Pasadena, USA, September 2008, pp. 1-3.

[10] DeLisio, M.P. and York, R.A.: “Quasi-Optical and Spatial Power Combining”, IEEE Trans. MTT, 2002, 50 (3), pp. 929-936.

[11] Rosenau, S.A., *et al*.: “High efficiency frequency multiplier grid arrays for watt-level millimeter wave sources”, IEEE Int. Vacuum Electronics Conf., 2002, pp. 202–203.

[12] Hwu, R. J., Sadwick, L. P., Luhmann, N. C. Jr., Rutledge, D. B., Sokolich, M., Hancock, B.: "Quasi-Optical Watt-Level Millimeter-Wave Monolitic Solid-State Diode-Grid Frequency Multipliers", Microwave Symposium Digest, IEEE MTT-S International, 1989, 3, pp. 1069 – 1072.

[13] Cryan, M., Helbing, S., Alimenti, F, Mezzanotte, P., Roselli, L., and Sorrentino, R.: "Simulation and Measurement of Quasi-Optical Multipliers", IEEE Trans. MTT, 2001, 49, (3), pp. 451-464.

[14] Moussessian, A., Wanke, M. C., Li, Y., Chiao, J.-C., Allen, S. J., Crowe, T. W., and Rutledge, D. B.: "A Terahertz Grid Frequency Doubler", IEEE Transactions on Microwave Theory and Techniques, 1998, 46, (11), pp. 1976-1981.

[15] Ortiz, S. C., Ivanov, T., and Mortazawi, A.: "A CPW-Fed Microstrip Patch Quasi-Optical Amplifier Arrays", IEEE Trans. Microwave Theory & Tech., 2000, MTT-48, (2), pp. 276-280.

[16] Maestrini, A., Ward, J. S., Gill, J. J., Javadi, H. S., Schlecht, E., Tripon-Canseliet, C., Chattopadhyay, G., and Mehdi, I.: "A 540–640-GHz High-Efficiency Four-Anode Frequency Tripler", IEEE Transactions on Microwave Theory and Techniques, 2005, 53, (9), pp. 2835-2843.

[17] Pigeon. M, Donnan. R, Dubrovka. R, Kreouzis. T, Wang. H, Alderman. B, Huggard P. G.: “Planar quasi-optic THz source: The multenna”, 2015 IEEE International Symposium on Antennas and Propagation & USNC/URSI National Radio Science Meeting, Vancouver, Canada, July 2015, pp. 2123-2124.

[18] Pigeon. M, Donnan. R, Kreouzis. T, Parini. C, Dubrovka. R.: “Improving Harmonics’ Generation by “zeroing- Stubs” in a Slot-Ring Antenna”, European Conference on Antenna and Propagation, Davos, Switzeland, April 2016, pp. 1-4.

[19] Alderman, B., Sanghera, H., Henry, M., Wang, H., Wilkinson, P., Williamson, D., Emery, M. and Matheson, D.: “Schottky Diode Technology at the Rutherford Appleton Laboratory”, proc. of the 2nd UK/Europe-China Conference on Millimetre Waves and Terahertz Technologies, Oxford, UK, October 2009, pp. 4-6

[20] Churilova S. A., Schuenemann K. and Vavriv D.M.: “Potentials of the clinotron for high-power high-frequency generation”, Proc. of the 28th European Microwave Conference, Amsterdam, October 1998, pp. 300-305.

[21] Siles, J. V. and Grajal, J.: "Physics-Based Design and Optimization of Schottky Diode Frequency Multipliers for Terahertz Applications", IEEE Transactions on Microwave Theory and Techniques, 2010, 58, (7), pp. 1933-1942.

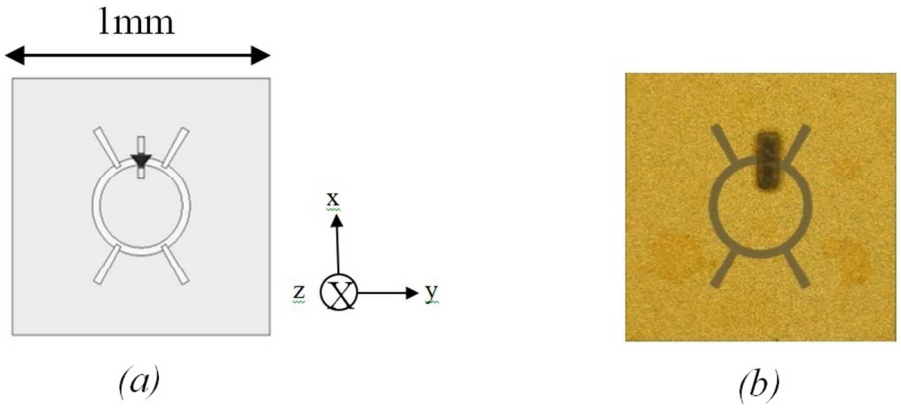

Fig. 1: One possible design of the multenna, termed "ET": it is a modified slot ring with stubs to enhance third harmonic yield. (a) Shows a schematic of the antenna and, (b) is a photograph of the manufactured antenna. The grey rectangle in (b) is the chip that carries the Schottky diode.

268x121mm (96 x 96 DPI)

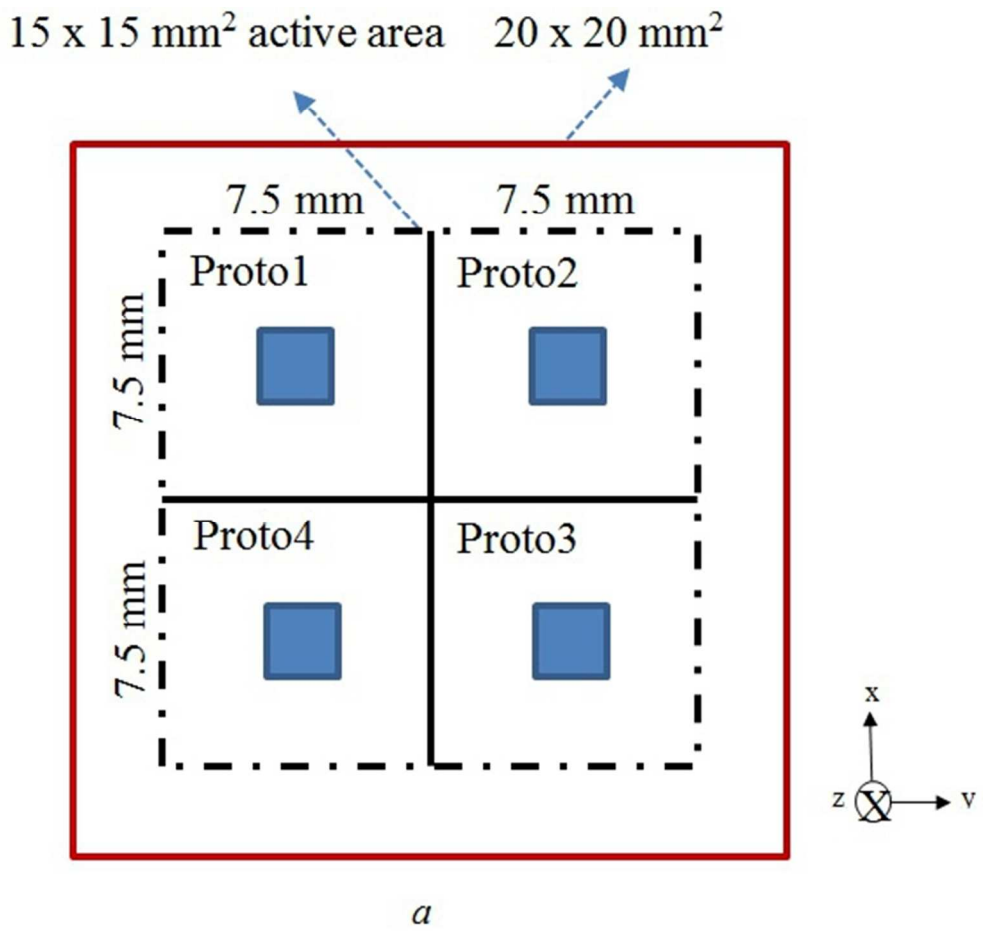

Fig. 2: Schematic of the quartz tile upon which four prototypes of the multenna are set.

151x140mm (96 x 96 DPI)

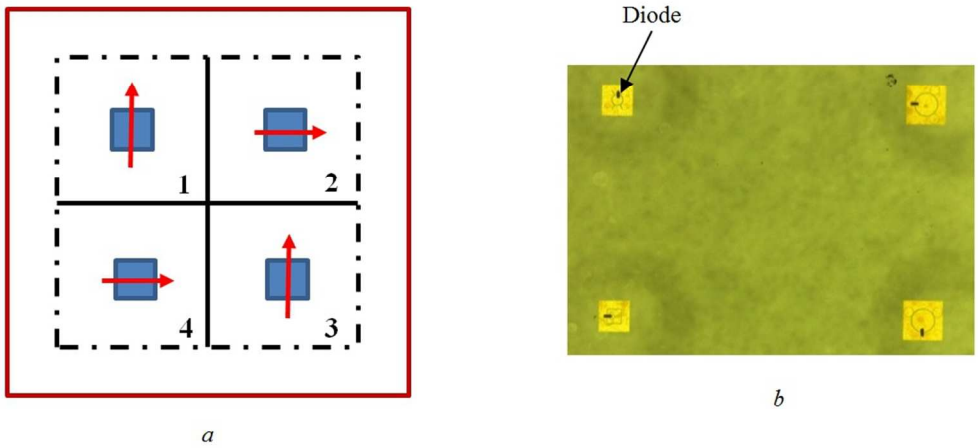

Fig. 4: a) Orientation for the polarization of the E-field for each prototype on the quartz tile and b) the actual display on the quartz tile with diodes (black rectangles), indicating the polarization orientation.

288x129mm (96 x 96 DPI)

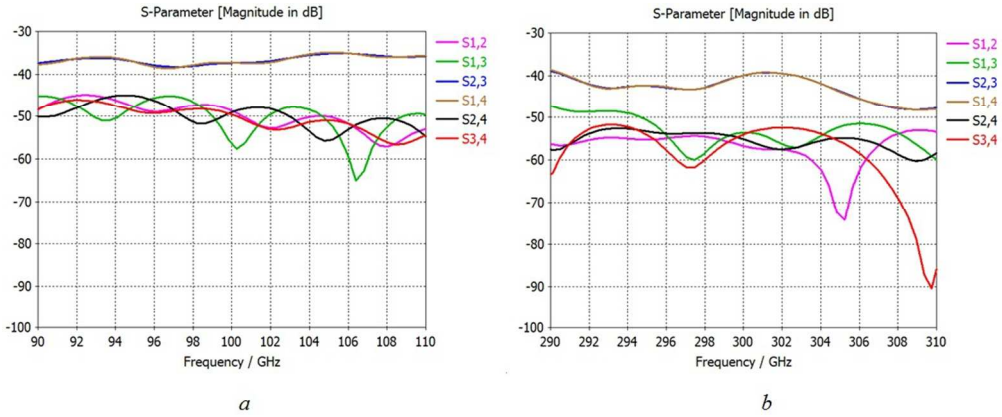

Fig. 5: S parameters for each multenna prototype on the tile a) at 100 GHz and b) 300 GHz.

308x126mm (96 x 96 DPI)

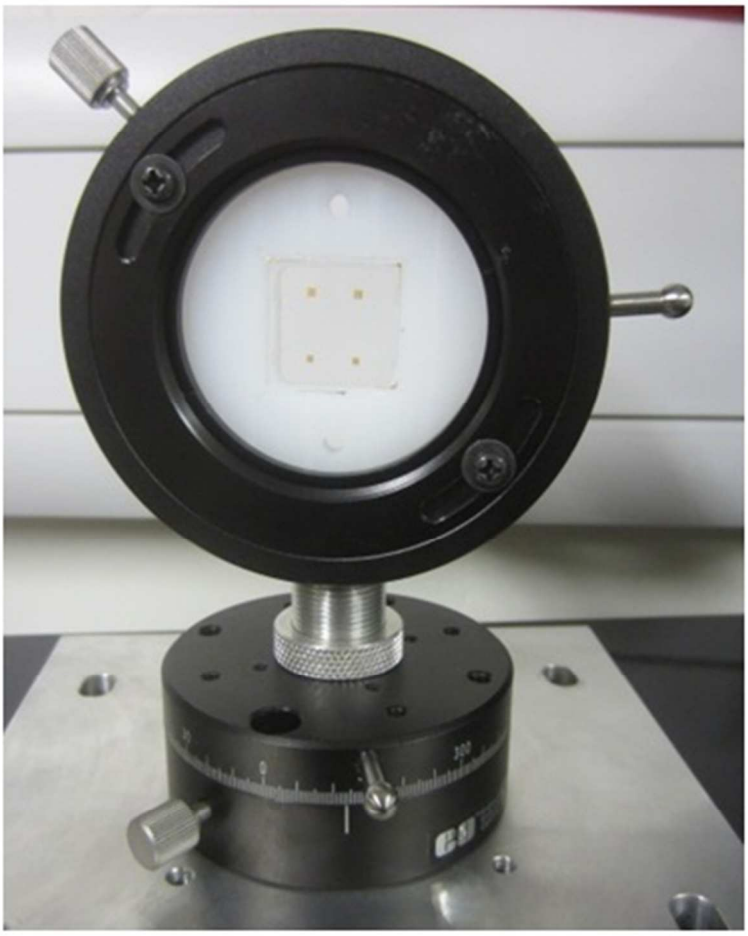

Fig. 6: The sample with four multennas on a quartz tile fixed in the rotating holder.

101x125mm (96 x 96 DPI)

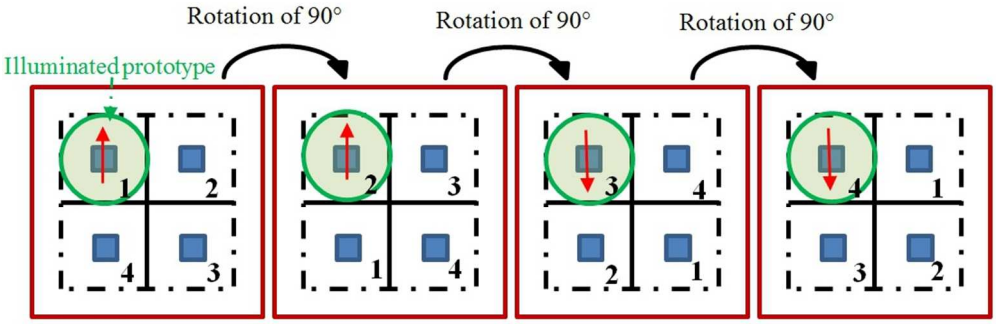

Fig. 7: The measurement procedure for characterising each prototype antenna in turn for a given polarisation condition by rotating the holder of the tile.

292x125mm (96 x 96 DPI)

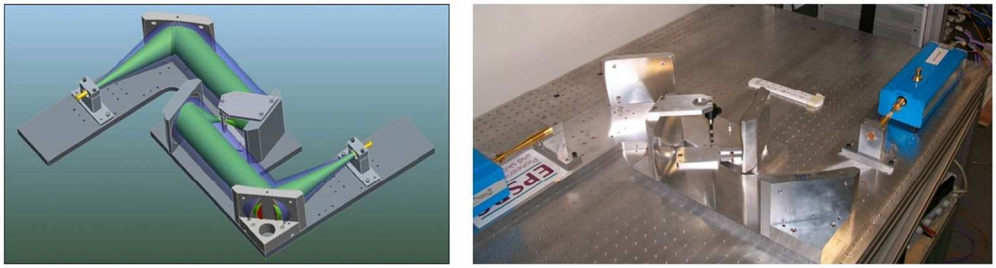

Fig. 8: Schematics (left) and a picture (right) of the quasi-optical Z-bench incorporating an inner pair of confocal mirrors braced by off-axis ellipsoidal coupling mirrors.

318x85mm (96 x 96 DPI)

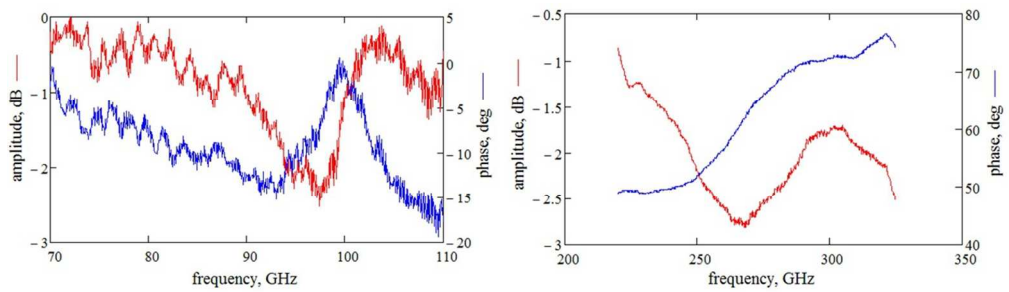

Fig. 9: Transmission measurements of the single multenna element in WR-10 and WR-3 waveguide bands normalised to the corresponding transmission of the quartz dielectric. Red lines show amplitude data, blue indicates phase.

346x100mm (96 x 96 DPI)

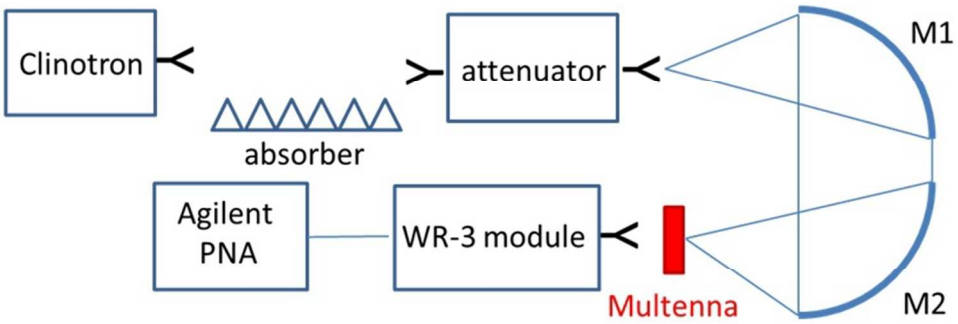

Fig. 10: Schematic of the measurement setup for testing of the frequency tripling performance of the multenna

226x85mm (96 x 96 DPI)